

## Determination of the Structure of Hydrogen on a W(211) Surface

O. Grizzi, M. Shi, H. Bu, and J. W. Rabalais

Department of Chemistry, University of Houston, Houston, Texas 77204-5641

R. R. Rye

Division 1124, Sandia National Laboratory, Albuquerque, New Mexico 87185

P. Nordlander<sup>(a)</sup>

Department of Physics and Astronomy, Rutgers University, P.O. Box 849,  
Piscataway, New Jersey 08855-8549

(Received 8 May 1989)

Time-of-flight scattering and recoiling spectrometry is applied to structural analysis of hydrogen on a W(211) surface. Experimental data in the form of a recoiling structural contour map are presented and the hydrogen position is determined as  $0.58 \pm 0.20 \text{ \AA}$  above the first-layer W plane and confined within a band that is centered above the  $[1\bar{1}\bar{1}]$  troughs. Effective-medium-theory calculations predict a broad probability distribution for the H-atom positions above the troughs due to thermally activated vibrational motion.

PACS numbers: 68.35.Bs, 79.20.Nc, 82.65.My

Although hydrogen/metal systems have been extensively studied, there have been few studies of the binding geometry of hydrogen on metals. The technique of electron-energy-loss spectroscopy (EELS) has been the most successful in determining hydrogen binding sites.<sup>1,2</sup> The conventional technique for studying adsorbate binding sites, low-energy electron diffraction (LEED), has low sensitivity for hydrogen. Recently,<sup>3,4</sup> time-of-flight scattering and recoiling spectrometry (TOF-SARS) has been shown to be extremely sensitive to surface hydrogen and to have the potential for obtaining structural information.

This paper describes TOF-SARS and applies it to the elusive problem of the determination of adsorbed hydrogen structure, specifically hydrogen on W(211). The data used in the analysis are TOF spectra of hydrogen (neutral plus ion) recoiling intensities  $I_R$  stimulated by  $\text{Ne}^+$  and  $\text{Ar}^+$  projectiles, coupled with classical ion-trajectory simulations. The experimental H binding site is compared with theoretical calculations using the effective-medium theory (EMT).<sup>5</sup>

TOF-SARS is based on the classical behavior<sup>4,6</sup> of atomic collisions in the keV range where atoms scatter and recoil from the repulsive potentials of atomic cores, i.e., the nucleus plus core electrons. As a projectile ion approaches a target atom, the trajectories are bent such that an excluded volume, i.e., a *shadow cone*, in the shape of a paraboloid is formed behind the target atom. The deflected trajectories are focused (Fig. 1) at the edge of these shadow cones, whose radii are of the order of  $\sim 1 \text{ \AA}$ , making the technique sensitive to the outermost atomic layers of a surface.

Light adsorbates can be sensitively detected by recoiling them into a forward angle  $\phi$ . As the beam-surface incident angle  $\alpha$  increases, a critical value,  $\alpha_c$ , is reached where the adsorbate atoms move out of their neighboring

atom shadow cones so that direct collisions with incident ions are possible.<sup>7</sup> Two types of events, *direct recoils* (DR) and *surface recoils* (SR), are possible as shown in Fig. 1. DR events occur when the value of the impact parameter ( $p$ ) below the adsorbate atom is accessible for single-collision recoil into a specific  $\phi$ . SR events occur when neighboring atoms focus the projectiles at a  $p$  value above the adsorbate atom such that it is recoiled down

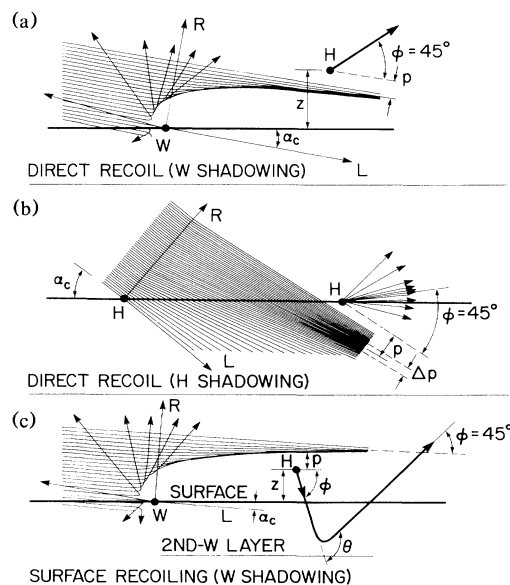


FIG. 1. Trajectory simulations of direct recoil (DR) and surface recoil (SR) of H atoms by 2-keV  $\text{Ne}^+$  ions illustrating (a) DR and focusing by W atoms, (b) DR and focusing by H atoms, and (c) SR and focusing by W atoms.  $\text{Ne}^+$  trajectories penetrate into the H "cone" in (b) and are concentrated at the "cone edge," resulting in a spread of  $\Delta p = 0.09 \text{ \AA}$  in  $p$ .

onto the substrate lattice and subsequently scatters into  $\phi$ . Focusing at the shadow cone edges produces sharp well-defined peaks in  $I_R$  as a function of  $\alpha$ . Rotating the crystal about its azimuthal angle  $\delta$ , i.e., about the surface normal, aligns the ion beam with other azimuths with different interatomic spacings, resulting in different  $\alpha_c$  values. By measuring  $\alpha_c$  corresponding to the recoil event, the interatomic distance of the adsorbate atom from its nearest neighbor along the trajectory can be determined from  $p$  and the shape of the shadow cone, i.e., the radius ( $R$ ) as a function of distance ( $L$ ) behind the target atom. The interatomic spacings between the adsorbate atom and first- and second-layer atoms can then be directly determined<sup>6</sup> from simple geometry.

The recoiled atoms can be identified by their TOF at fixed  $\phi$  due to their high, discrete velocity distributions which are well described<sup>4</sup> by classical mechanics. For an incident ion of mass  $M_1$  and energy  $E_0$ , the TOF of a target atom of mass  $M_2$  that undergoes DR into an angle  $\phi$  is

$$t_{DR} = l(M_1 + M_2)/(8M_1E_0)^{1/2} \cos\phi, \quad (1)$$

where  $l$  is the flight distance. A continuous-angle TOF-SARS spectrometer and TOF spectral acquisition have been described previously.<sup>4,6</sup> Since the TOF technique is an efficient multichannel collection method which is capable of directly detecting both recoiled ions and fast neutrals (most of the recoils are neutrals) directly in a channel electron multiplier, it is a nondestructive analysis method. The parameters used herein are the following: 2–5-keV  $\text{Ne}^+$  or  $\text{Ar}^+$  primary beam; pulse width of beam, 30 nsec; pulse rate, 1–50 kHz; average current density, 0.05–0.1 nA/mm<sup>2</sup>; signal rate up to  $\approx 15000$  counts/sec; TOF flight path, 98.4 cm;  $\text{H}_2$  dose, 10 L [1 L (langmuir) =  $10^{-6}$  Torrsec]. TOF spectra can be acquired in  $\approx 20$  sec, resulting in a dose of  $\approx 10^{-4}$  ions/(surface atom). The W(211) surface consists (see Fig. 4) of parallel close-packed rows of atoms separated by channels; thermal desorption measurements<sup>8</sup> have suggested that there is a  $\beta_2$  state located in the troughs and a  $\beta_1$  state above the rows. Spectra were collected with the sample in the range 340–450 K in order to assure population of only the  $\beta_2$  state.<sup>8</sup> The azimuthal directions are defined as follows:  $\delta = 0^\circ$  (perpendicular to rows) is  $[01\bar{1}]$ ;  $\delta = \pm 90^\circ$  (parallel to rows) is  $[\bar{1}11]$  and  $[1\bar{1}\bar{1}]$ .

Classical trajectory simulations,<sup>9</sup> using screened Coulomb potentials, are used to trace the trajectories and map out the cones (Fig. 1). Higher accuracy is achieved by calibrating<sup>6</sup> the potential; this involves measuring  $\alpha_c$  values along crystal azimuths for which the interatomic distances  $d$  are accurately known and using these values to determine the experimental  $R$  of the cone at different  $L$  values. The screening constant of the potential is then adjusted so that the standard deviation of the calculated cone from the experimental points on a

plot of  $R$  vs  $L$  is minimized. TOF spectra<sup>4</sup> are collected and the recoil spectral peak intensities  $I_R$  (measured as the TOF peak area) are determined as a function of  $\alpha$  and  $\delta$ . SR and DR peaks are deconvoluted at low  $\alpha$ . The ability to continuously vary  $\phi$  is important in order to obtain a suitable  $\phi$  where the recoiling and scattering peaks do not overlap. Collecting  $I_R$  data as a function of  $\alpha$  probes the ability of the incident ions to hit adsorbate sites. Collecting  $I_R$  data as a function of  $\delta$  illustrates (i) the symmetry of the adsorbate positions and (ii) the azimuths along which the recoil channel is accessible or obstructed.

Data for  $\text{H}_2$  adsorption on W(211) are shown in Fig. 2 as a recoiling structural contour map (RSCM). It represents  $I_R$  data in  $\alpha, \delta$  space; contour lines connect points of equal intensity. The RSCM provides the following information. (i) It is a concise summary of the experimental recoil data. (ii) It reveals the symmetry of the recoil data in  $\alpha, \delta$  space, providing a *fingerprint* for hydrogen on the W(211) surface. (iii) Changes in the minimum  $\alpha_c$  value reveal azimuths along which the shadowing conditions differ, i.e., shadowing of H atoms by neighboring H or W atoms differs. At low  $\alpha$  a sharp rise in  $I_R$  is observed in Fig. 2; its constant position (near  $\alpha_c = 4^\circ - 5^\circ$ ) over  $-85^\circ < \delta < +85^\circ$  indicates that H is rather uniformly accessible to the beam in relatively high positions above the surface. At  $\delta = \pm 90^\circ$  the  $I_R$  maximum occurs at  $\alpha \sim 18^\circ$  ( $\alpha_c = 10^\circ$ ) signifying close packing<sup>6</sup> along this direction. There is a large, relatively flat, featureless region in the center and background of the RSCM. This indicates that there is no H buried deep in the troughs that is accessible for recoiling.

Hydrogen atoms in on-top or short-bridge positions

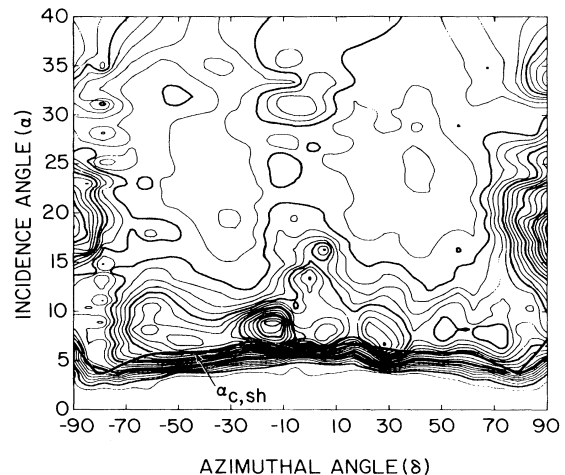


FIG. 2. Recoiling structural contour map for the W(211)-H surface using 4-keV  $\text{Ar}^+$  ions and  $\phi = 45^\circ$ . The  $\alpha_c$  value, chosen at one-half the peak height, is plotted as a heavy line. Regions with high contour densities represent maxima in  $I_{DR}$ .

above the  $[1\bar{1}\bar{1}]$  rows would be in such high positions (the normal H-W bond length<sup>10</sup> is in the range 1.74–1.95 Å) that they would be well outside of the Ne/W and Ar/W shadow cones which have radii<sup>4</sup> in the range 0.95–1.30 Å, respectively. As a result, the sharp rises observed in Fig. 2 at low  $\alpha$  would not be present because the cone edges would not move through the H-atom positions; instead, a rather uniform  $I_R$  would be observed as a function of  $\alpha$ . The only H-atom positions that are consistent with all of the data (as detailed elsewhere<sup>6</sup>) are located within a band above the  $[1\bar{1}\bar{1}]$  troughs. Shadowing of H in this position along  $-85^\circ < \delta < +85^\circ$  directions is due to neighboring first-layer W atoms and along  $\delta = \pm 90^\circ$  is due to neighboring H atoms. We now consider determination of the adsorption-site coordinates.

**[211] coordinate, i.e., perpendicular to plane of first-layer W atoms.**—The low  $\alpha_c$  values,  $4^\circ$ – $5^\circ$ , for  $-85^\circ < \delta < +85^\circ$  are due to SR events resulting from focusing of projectile trajectories above the H atoms by first-row W atoms (Fig. 1). At such low  $\alpha$  values, the edge of the W-atom shadow cone is relatively flat above the trough such that H atoms located at a given height  $z$  but different lateral positions within the trough all appear at the same  $\alpha_c$  value within  $\approx 0.5^\circ$ . However, changes of only 0.1 Å in  $z$  produce changes in  $\alpha_c$  of as much as  $2^\circ$ – $3^\circ$ . This feature can be used to determine  $z$  as follows. Because of the  $\cos^2\phi$  dependence of the DR energy and the insensitivity of the H scattering energy to scattering angle  $\Theta$  (H loses  $< 2\%$  of its energy during

reflection from the W lattice), the final energy (and TOF) of SR H atoms is determined mainly in the initial projectile-H collision and can be calculated from Eq. (1) as a function of  $\alpha$  and  $z$ . The best agreement between the experimental and calculated TOF vs  $\alpha$  curves using 2- (see Fig. 3) and 5-keV Ar<sup>+</sup> yielded  $z = 0.60$  and  $0.55$  Å, respectively.

**H-H interatomic distance along the  $[1\bar{1}\bar{1}]$  trough.**—Along this azimuth,  $\alpha_c$  is determined by the self-shadowing of incident projectile trajectories by H atoms, since the H atoms are high enough above the second-layer W atoms to be well outside of the W-atom shadow cones. The Ne trajectories penetrate into the H-atom “shadow cone;” the presence of H causes the trajectories to diverge<sup>6</sup> sufficiently such that they concentrate at the “cone edge.” This cone edge is not sharp as in the case of a heavy target atom. Note the gentle slope at  $\delta = 90^\circ$  and steep slope at  $\delta = 0^\circ$  in Fig. 3. DR of H atoms into  $\phi$  occurs when the cone edge is at a distance equal to the appropriate  $p$  below the atom. Using the  $\alpha_c = 10^\circ$  (Fig. 3),  $p = 0.13$  Å for H DR into  $45^\circ$ , and the calculated extremities ( $R = 0.29$  Å and  $0.38$  Å) of the cone edge, the H-H distance can be varied until the perpendicular distance from the neighboring H atom to the center of the cone is  $p + R$ . The best fit is obtained<sup>6</sup> for an H-H spacing of  $\approx 2.7$  Å, in excellent agreement with the W-W lattice spacing of 2.74 Å along  $\delta = \pm 90^\circ$  and, therefore, a coverage of one H atom per W lattice spacing. The low  $\alpha_c$  value ( $\alpha_c = 5^\circ$ ) along the  $\delta = 0^\circ$  azimuth indicates that H atoms are too far apart to be aligned within the same trough. This result is consistent with one H atom per trough along the  $\delta = 0^\circ$  direction for a saturation coverage of  $\sim 8 \times 10^{14}$  atoms/cm<sup>2</sup>.

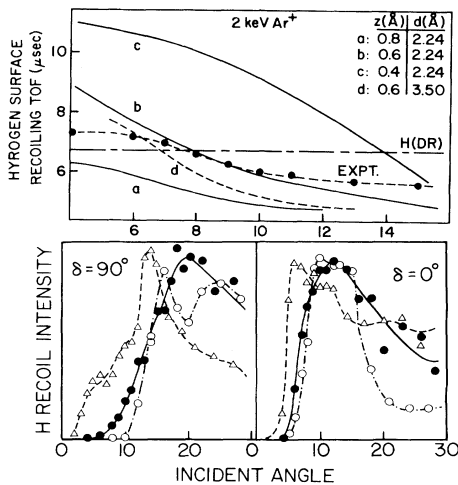


FIG. 3. Lower: Incident-angle scans of H recoil intensity. The steep slope and low  $\alpha_c$  for  $\delta = 0^\circ$  are due to focusing by W atoms (SR events) and the gentle slope and higher  $\alpha_c$  for  $\delta = 90^\circ$  are due to focusing by H atoms (DR events). Triangles, 5-keV Ne<sup>+</sup>; closed circles, 2-keV Ne<sup>+</sup>; open circles, 2-keV Ar<sup>+</sup>. Upper: Calculated TOF vs  $\alpha$  curves for H DR and SR (a–d) into  $\phi = 45^\circ$  compared to experimental TOF using 2-keV Ar<sup>+</sup> along the  $\delta = 0^\circ$  azimuth.

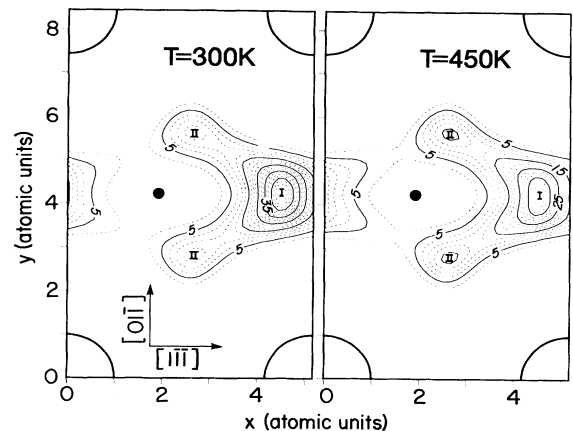


FIG. 4. Contour plot of  $P^{\text{tot}}$  [Eq. (3)] for  $T = 300$  and  $450$  K.  $P^{\text{tot}}$  is normalized to 100. The solid and dashed lines represent increments of 10 and 2.5 units of  $P$ , respectively. The open circles at the corners represent first-layer W atoms and the closed circle in the center represents a second-layer W atom; the atomic sizes are not scaled to the W radius. I denotes the short-bridge and II the threefold trough sites.

We have shown that the  $\beta_2$  form of hydrogen on W(211) is confined to a band located at 0.58 Å above the troughs with an average H-H spacing equal to that of the W lattice. In order to determine the specific adsorbate site from recoiling, the adsorbed species must be localized to a volume smaller than the shadow cone. These conditions are met in the case of oxygen on W(211) where a definite site (the threefold trough site) is determined,<sup>6</sup> but clearly not met in the case of hydrogen; the results indicate that H is delocalized along the troughs.

The equilibrium distribution of H on W(211) using a potential-energy surface generated by the effective-medium theory<sup>5</sup> has been calculated. The Schrödinger equation was numerically integrated using the relaxation method.<sup>11-13</sup> The resulting H-W potential is shallow, with a barrier to motion along the  $[\bar{1}\bar{1}\bar{1}]$  troughs of only 100 meV. The lowest excited states correspond to vibrations parallel to the surface which have large amplitudes, fill a large portion of the trough, and can be populated thermally. The probability for finding the H atom at position  $R$  in the unit cell can be obtained from the thermal average

$$P(R, T) = \frac{\sum_k e^{-\beta E_k} |\psi_k(R)|^2}{\sum_k e^{-\beta E_k}}, \quad (2)$$

where  $\beta = 1/k_B T$  and  $E_k$  is the energy of excited state  $k$ . All nonpropagating excited states (total of 10) with  $E_k < 77$  meV are included in the summation.<sup>6</sup>  $P(R, T)$  is finite over the entire unit cell; i.e., the H atom exists within a band above the trough. This band extends vertically from 0.4 to 0.8 Å above the first W layer, with a most probable distance of 0.60 Å. At 0 K, only the ground state would contribute to the sum of Eq. (2) and  $P(R)$  would be localized. The total probability,  $P^{\text{tot}}(x, y)$ , of finding a H atom at lateral position  $x, y$  is

$$P^{\text{tot}}(x, y, T) = \int dz P(x, y, z, T). \quad (3)$$

A contour plot of  $P^{\text{tot}}(x, y)$  for  $T = 300$  and 450 K in a surface unit cell is shown in Fig. 4.  $P^{\text{tot}}$  is finite throughout the unit cell with maxima at the short-bridge and threefold trough sites,<sup>6</sup> but exhibiting large-amplitude vibrations about these positions. Thus, the

calculations show that at 450 K, H atoms are delocalized<sup>11,14</sup> to a greater extent than the W shadow-cone radius.

In summary, TOF-SARS is capable of detecting surface hydrogen with high sensitivity and providing a real-space determination of its adsorption site. Coupling these data with EMT calculations provides a powerful probe of hydrogen-surface interactions.

This material is based upon work supported by the National Science Foundation under Grants No. CHE-8814337 and No. DMR-88-01027 and the Texas Advanced Research Program.

(a)Permanent address: Department of Physics, Rice University, Houston, TX 77251.

<sup>1</sup>W. Ho, R. F. Willis, and E. W. Plummer, Phys. Rev. Lett. **40**, 1463 (1978).

<sup>2</sup>G. B. Blanchet, N. J. DiNardo, and E. W. Plummer, Surf. Sci. **118**, 496 (1982).

<sup>3</sup>B. J. J. Koeleman, S. T. de Zwart, A. L. Boers, B. Poekema, and L. K. Verheij, Phys. Rev. Lett. **56**, 1152 (1986).

<sup>4</sup>J. W. Rabalais, CRC Critical Rev. Solid State Mater. Sci. **14**, 319 (1988).

<sup>5</sup>P. Nordlander, S. Holloway, and J. K. Norskov, Surf. Sci. **136**, 59 (1984).

<sup>6</sup>O. Grizzi, M. Shi, H. Bu, and J. W. Rabalais (to be published).

<sup>7</sup>M. Aono and R. Souda, Jpn. J. Appl. Phys. **24**, 1249 (1985).

<sup>8</sup>P. G. Cartier and R. R. Rye, J. Chem. Phys. **59**, 4602 (1973); R. R. Rye, B. D. Barford, and P. G. Cartier, J. Chem. Phys. **59**, 1693 (1973).

<sup>9</sup>S. R. Kasi, M. A. Kilburn, H. Kang, J. W. Rabalais, L. Tavernini, and P. Hochmann, J. Chem. Phys. **88**, 5902 (1988).

<sup>10</sup>K. A. R. Mitchell, Surf. Sci. **149**, 93 (1985); R. Biswas and D. R. Hamann, Phys. Rev. Lett. **56**, 229 (1981).

<sup>11</sup>M. J. Puska, R. M. Nieminen, M. Manninen, B. Chakraborty, S. Holloway, and J. K. Norskov, Phys. Rev. Lett. **51**, 1081 (1983).

<sup>12</sup>D. R. Hamann and P. J. Feibelman, Phys. Rev. B **37**, 3847 (1988).

<sup>13</sup>G. E. Kimball and G. H. Shortley, Phys. Rev. **45**, 815 (1934).

<sup>14</sup>I. Stensgaard and F. Jakobsen, Phys. Rev. Lett. **54**, 711 (1985).